RECENT COMMISSIONING RESULTS FROM THE SPALLATION NEUTRON SOURCE*

Stuart Henderson, representing the commissioning team, Spallation Neutron Source Project, Oak Ridge National Laboratory, Oak Ridge TN, USA

Abstract

The Spallation Neutron Source accelerator complex consists of a 2.5 MeV H^- front-end injector system, a 186 MeV normal-conducting linear accelerator, a 1 GeV superconducting linear accelerator, an accumulator ring and associated beam transport lines. The beam commissioning campaign of the SNS accelerator complex, initiated in 2002 and completed in May 2006, was performed in seven discrete runs as each successive portion of the accelerator complex was installed. The final beam commissioning run, in which beam was transported to the liquid mercury target was recently completed. In the course of beam commissioning, most beam performance parameters and beam intensity goals have been achieved at low duty factor. The beam performance and beam dynamics measurements of the linac and ring are described.

INTRODUCTION

The Spallation Neutron Source (SNS) is a short-pulse neutron scattering facility under construction at Oak Ridge National Laboratory by the U.S. Department of Energy. The SNS construction project was a partnership of six US DOE national laboratories, each of which had responsibility for designing and manufacturing a portion of the facility. At 1.44 MW of proton beam power on target, the SNS will operate at beam powers a factor of 7 beyond that which has been previously achieved [1]. The SNS baseline parameters are summarized in Table 1.

Table 1: SNS Design Parameters

Beam Power on Target	1.44 MW
Beam Energy	1.0 GeV
Linac Beam Macropulse Duty Factor	6.0%
Beam Pulse Length	1.0 msec
Repetition Rate	60 Hz
Chopper Beam-On Duty Factor	68%
Peak macropulse H- current	38 mA
Average Linac H- current	1.6 mA
Ring accumulation time	1060 turns
Ring bunch intensity	1.6×10^{14}
Ring Space-Charge Tune Spread	0.15
Beam Pulse Length on Target	695 nsec

The SNS accelerator complex [2] consists of a 2.5 MeV H^- injector [3], a 1 GeV linear accelerator [4], an accumulator ring and associated beam transport lines [5]. The injector (also called the Front-End Systems) consists of an H- volume ion-source with 50 mA peak current capability [6], a Radio-Frequency Quadrupole and a Medium Energy Beam Transport line for chopping and matching the 2.5 MeV beam to the linac. The linear accelerator consists of a Drift Tube Linac (DTL) with 87 MeV output energy, a Coupled-Cavity Linac (CCL) with 186 MeV output energy, and a Superconducting RF Linac (SCL) with 1 GeV output energy [7]. The linac produces a 1 msec long, 38 mA peak, chopped beam pulse at 60 Hz for accumulation in the ring.

The linac beam is transported via the High Energy Beam Transport (HEBT) line to the injection point in the accumulator ring, where the 1 msec long pulse is compressed to less than 1 microsecond by charge-exchange multi-turn injection. According to design, beam is accumulated in the ring over 1060 turns reaching an intensity of 1.5×10^{14} protons per pulse. When accumulation is complete the extraction kicker fires during the 250 nsec gap to remove the accumulated beam in a single turn and direct it into the Ring to Target Beam Transport (RTBT) line, which takes the beam to a liquid-mercury target.

Staged commissioning of the accelerator complex, now complete, was performed in 7 discrete beam commissioning runs, as shown in Figure 1. The 7 runs were devoted to commissioning the i) front-end, ii) Drift Tube Linac Tank 1, iii) Drift Tube Linac Tanks 1-3, iv) Coupled Cavity Linac, v) Superconducting linac, vi) High-Energy Beam Transport Line and Accumulator Ring, and vii) Ring to Target Beam Transport Line and the mercury target. Table 2 summarizes the main beam commissioning results, comparing beam measurements with design goals.

With the construction project complete, the SNS is now transitioning to user-mode operations.

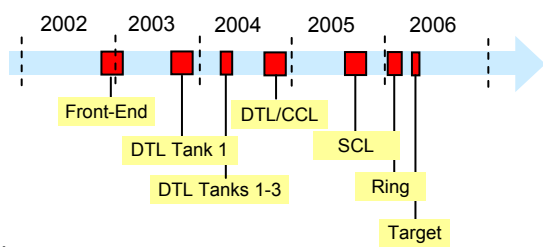

Figure 1: SNS Beam Commissioning Schedule

BEAM COMMISSIONING TOOLS

Beam Diagnostic Systems

An overview of SNS diagnostic systems is given in [8]. The front-end diagnostic systems are utilized to quantify the linac input beam parameters. Systems include an inline x-y emittance station, a mode-locked laser system

*SNS is managed by UT-Battelle, LLC, under contract DE-AC05-00OR22725 for the U.S. Dept. of Energy. SNS is a partnership of six national laboratories: Argonne, Brookhaven, Jefferson, Lawrence Berkeley, Los Alamos and Oak Ridge.

for longitudinal profile measurements, beam position and current monitors. The normal conducting linac includes energy degrader/faraday cups located after each DTL tank, beam loss monitors, beam position and current monitors, and a set of bunch-shape monitors [9] for longitudinal profile measurements at the entrance to the CCL. The superconducting linac includes beam loss, position and current monitors as well as a laser-based transverse profile measurement system [10].

Table 2: Beam parameters achieved in commissioning

Parameter	Design	Measured
Linac Transverse Output Emittance [π mm-mrad (rms, norm)]	0.4	0.3 (H) 0.3 (V)
CCL1 Bunch Length [deg]	3	4
Linac Peak Current [mA]	38	>38
Linac Output Energy [MeV]	1000	952
Linac Average Current [mA]	1.6	1.05 (DTL1) 0.004 (SCL)
Linac H-/ions/pulse	$1.6x10^{14}$	$1.0x10^{14}$
Linac pulse length/rep rate/duty factor [msec/Hz/%]	1.0/60/6.0	1.0/60/3.8 (DTL1) .050/1/.005 (CCL) 0.85/0.2/.01 7 (SCL)
Ring intensity	$1.5x10^{14}$	$1.0x10^{14}$ (unbunched)
Extracted beam intensity	$1.5x10^{14}$	$5.0x10^{13}$
Beam intensity on target	$1.5x10^{14}$	$1.8x10^{13}$

The ring and transport line diagnostic systems include beam loss, current and position monitors, wire scanners in the transport lines, and a harp system located 10m before the mercury target. For the target commissioning run a temporary view screen was mounted to the front face of the target to verify the target beam profile and validate injection painting.

Application Programs

Central to the success of the rapid beam commissioning of the SNS accelerator complex was a set of applications programs which were tested and available on day one of each commissioning phase. The XAL programming infrastructure [11] provided a powerful framework for rapid development and deployment of application programs. Approximately 50 application programs have been developed for commissioning and operation of the SNS accelerator complex. The SNS commissioning strategies and tuneup algorithms, expressed as XAL programs, are described elsewhere in these proceedings [12].

Many of the commissioning algorithms rely heavily on accurate real-time modelling of the accelerator. An online-model of the linac has been developed [11] which includes centroid tracking through individual RF gaps [13] to obtain the beam centroid arrival phase. Beam sizes are determined using an envelope approach [14]. Transport line modelling is also contained within the linac model. The linac model has been successfully benchmarked to Trace-3D and PARMILA. The Ring model at present consists of a linear, transport-matrix based model ignoring space-charge. This model is adequate for most of the commissioning operations since low-intensity beams are used for initial tuneup. The ring model has been successfully benchmarked to MAD and TRANSPORT.

LINAC COMMISSIONING RESULTS

Normal-conducting linac beam commissioning results have been reported previously [15]; therefore, we emphasize the superconducting linac commissioning results in this paper.

Determination of RF Setpoints

There are a total of 95 RF phase and amplitude setpoints in the linac which must be determined. The determination of those setpoints relies on comparisons of measured data with model predictions. In the normal-conducting linac, RF setpoints are determined using the phase-scan signature matching [16] and "Delta-T" [17] techniques. In the phase-scan signature matching technique the difference in beam arrival phase at two BPMs downstream of the DTL tank or CCL module in question is recorded as a function of tank or module phase for a few different RF field amplitudes. While the small amplitude motion is linear, phase scans are performed over a wide range in cavity phase to make use of the non-linearity of large amplitude motion. The input beam energy, tank or module RF amplitude and relative beam/RF input phase are determined with a model based fit to data obtained at two or more RF amplitudes. Figure 2 shows an example, where the curve displays measured data and the points show the model result after fitting.

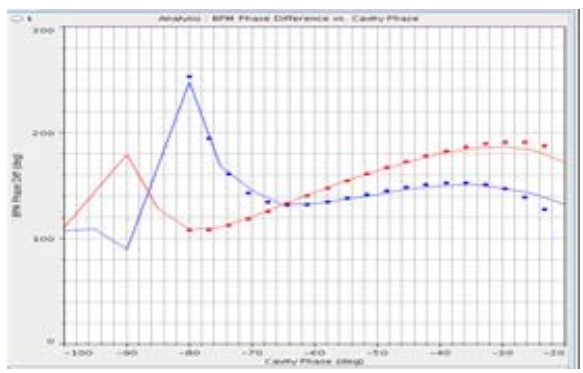

Figure 2: Results of phase-scan signature matching to determine RF setpoints. BPM phase difference is plotted vs. CCL module 2 phase. The curves show beam data for two RF amplitudes. The points show the results of model-based fitting.

The superconducting linac consists of 81 independently powered cavities. The principal method in use for determining RF setpoints is the well-known time-of-flight

based BPM phase scan. In this method the difference in beam arrival phase between two downstream BPMs is recorded as the SCL RF cavity phase is scanned across the full 360 degrees. The resulting phase difference is very nearly sinusoidal and is readily fit to obtain the input energy, the cavity accelerating gradient and the relative beam/cavity phase [18]. The cavity phase is set according to the measured relative beam/cavity phase and the design synchronous phase (which is typically -20 degrees). Figure 3 shows a sample measurement which is used to determine SCL RF setpoints.

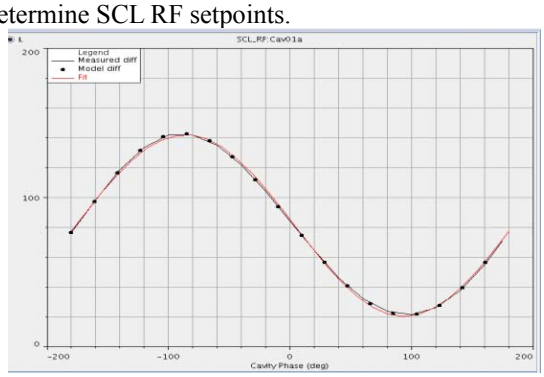

Figure 3: Downstream BPM phase difference vs. SCL cavity phase data (line) compared with results of model-based fitting (dots) and sinusoidal fitting (red).

A second method for determining cavity amplitudes and relative beam/RF phase utilizes the beam-induced signal generated by the beam drifting through an unpowered cavity [18].

A method for adjusting downstream cavity phases in response to an upstream cavity fault or setpoint change has been developed. Preliminary results are described elsewhere in these proceedings [12]. This method holds promise for rapid recovery from cavity faults, which will be necessary for achieving high availability in routine user-mode operation.

Transverse Dynamics

Proper transverse matching is essential to minimize emittance and halo growth driven by mismatch. Matching quadrupoles are available at the lattice transitions between MEBT and DTL, at the input to the CCL, between CCL and SCL, and between SCL and HEBT. Transverse matching is accomplished either by utilizing beam profile data to set matching quadrupoles, or by empirical adjustment of matching quadrupoles to minimize beam losses.

The most important linac beam quality measure is the transverse emittance growth. Sets of beam profile data from dual-plane wire scanner arrays in the CCL, SCL and HEBT allow measurement of the twiss parameters and transverse beam emittances. Gaussian fits to beam profile data were performed to obtain RMS beamsizes. Using a model-based fitting method and knowledge of the beam energy and quadrupole gradients, best-fit twiss parameters and RMS emittances were obtained. Table 3 shows results from a measurement campaign performed during SCL beam commissioning, showing that the emittance growth is consistent with the design specifications.

Table 3: Comparison of measured and expected RMS transverse beam emittances at four locations in the linac.

Location	**Measured ε_x, ε_y π-mm-mrad (rms, norm)**	**Design ε_x, ε_y π-mm-mrad (rms, norm)**
MEBT Entrance	0.22, 0.25	0.21
CCL Entrance	0.22, 0.25	0.33
SCL Entrance	0.27, 0.35	0.41
Linac Dump	0.26, 0.27	0.41

Linac Operation

The linac has operated thus far with output beam energies in the range 860-950 MeV. Linac beam current monitors for a typical beam pulse are shown in figure 4. This pulse has operating parameters as follows: 200 μs pulse length, 860 MeV, 18 mA peak current, 70% chopping duty factor, 12 mA average pulse current and 1.5×10^{13} H^- ions/pulse. Linac beam pulses as long as 880 μs, and with intensities as high as 1×10^{14} H^- ions/pulse have been obtained. A typical beam loss distribution is shown in Figure 5. The data show beam losses for a single beam pulse of 255 μs length and 2×10^{13} H^- ions/pulse. Peaks in the loss profile correspond to fractional losses of approximately 0.1% based on preliminary loss monitor response studies. Better loss performance in the linac/HEBT has been obtained in carefully established conditions; the data in the figure are typical of operating conditions during Ring beam commissioning. The elevated losses toward the end, in the injection dump line are due to beam interactions in the secondary stripping foil.

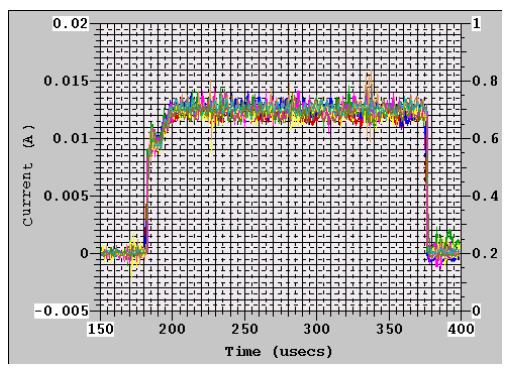

Figure 4: Overlay of beam current monitors in the linac for a typical beam pulse.

RING AND TRANSPORT LINE COMMISSIONING RESULTS

Ring Tuneup and Operation

Initial commissioning of the ring proceeded very rapidly, with first injection, ring circulation and extraction

accomplished over a four day period. Many of the ring setup operations are performed with a single "minipulse,"

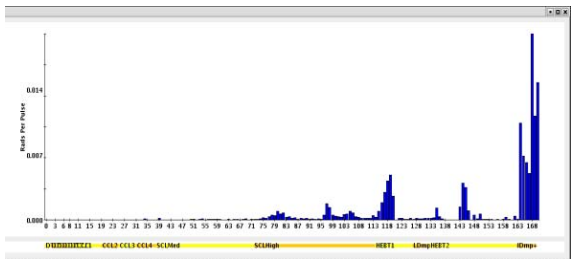

Figure 5: Beam loss profile for a single pulse from the MEBT through the linac and HEBT to the injection dump. Full scale is 0.021 rads/pulse. See text for details.

that is, a single train of linac microbunches sufficient to fill 70% of the ring circumference. Minipulses are formed by the LEBT and MEBT chopper systems which have risetimes of 40 nsec and 10 nsec respectively. During commissioning typically only the LEBT chopper was used during beam commissioning. The single minipulse signals are well-measured by the ring BPM system. Turn-by-turn data for a single circulating minipulse allow tune, closed-orbit, beta-function, dispersion and chromaticity measurements to be performed. Figure 6 shows a beam current monitor signal for a single minipulse circulating in the accumulator ring.

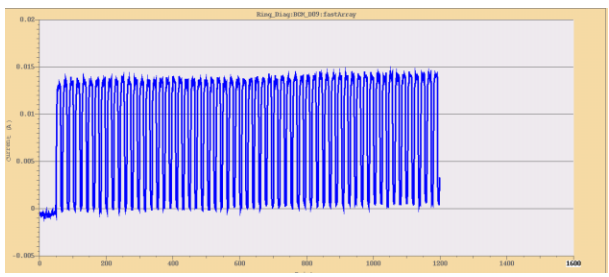

Figure 6: Ring beam current monitor data for a single circulating 13 mA minipulse.

Closed-orbit correction is accomplished with a model-based method. Figure 5 shows a resulting closed-orbit following correction. The large displacements show the dynamic injection bumps which are used for phase space painting.

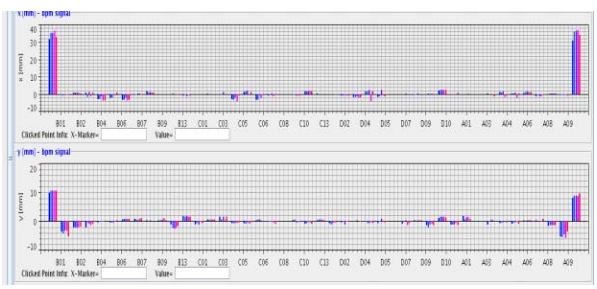

Figure 7: Horizontal (top) and vertical (bottom) closed orbits in the Ring. The vertical scales extend from -10 to +40mm (top) and -10 to +20mm (bottom).

Using the single minipulse turn-by-turn data the betatron phase advance between BPMs is measured. Figure 8 shows the difference between the measured and design horizontal betatron phase advance in the ring, together with a model-based fit, showing that the linear lattice is rather well-corrected, although small quadrupole string adjustments of 1-2% relative to the design values were made to correct the tunes. The measured natural chromaticities agree very well with design values. The measured values are -8.2 (horizontal) and -7.2 (vertical) whereas the design values are -7.9 and -6.9.

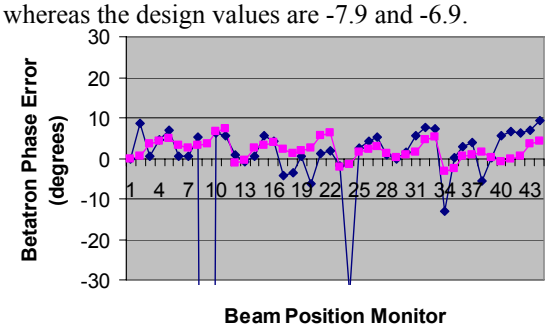

Figure 8: Horizontal betatron phase advance data (measured-design; blue) and a model-based fit (violet).

High-intensity Ring Studies

Accumulation in the ring has been tested for linac beam pulse lengths up to 400 μs in bunched beam mode, and up to 800 μs in coasting beam mode. Figure 9 shows the ring beam current monitor data for 180 turn accumulation of 1.6×10^{13} protons and subsequent extraction.

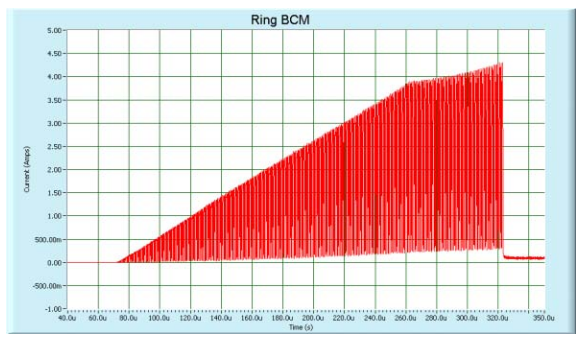

Figure 9: Ring beam current monitor data for 180 turn accumulation of 1.6×10^{13} protons/pulse.

In high-intensity studies, beam pulses up to 5×10^{13} protons/pulse were accumulated in bunched-beam mode with the ring RF system operating. The highest intensity yet achieved in the ring is 1×10^{14} protons per pulse in un-chopped, coasting beam mode. Figure 10 shows the beam current monitor signal, for the last five ring turns before extraction, of a bunch with 5×10^{13} protons. The longitudinal asymmetry is due to uncompensated beam-loading in the Ring RF system.

Collective beam instabilities were investigated during high intensity studies; the results are presented in detail elsewhere in these proceedings [19]. Thus far, no beam

instabilities have been observed in normal operating conditions with bunched beam and natural chromaticity. In order to explore beam instabilities in the accumulator ring, off-normal conditions were established: extraction was delayed to allow beam storage for tens of thousands turns to provide time for slow-growing modes, the chromaticity was set to zero in both planes, and coasting beams were stored.

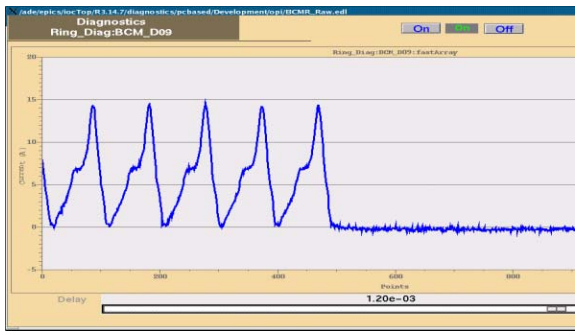

Figure 10: Ring beam current monitor data for the last five turns prior to extraction of a 5×10^{13} proton bunch.

The ring impedance is dominated by the fourteen ferrite-loaded extraction kickers [20]. In normal conditions at design intensity simulations predict a safety factor of 2-3 in the extraction kicker impedance before developing an instability. Simulations also predict the most unstable modes to be in the 5-10 MHz range. In off-normal conditions described above an instability was observed with ~1 msec growth time and dominant frequency at ~6 MHz. The driving impedance was determined from the measured growth rate and found to be 28 kΩ/m, compared to the estimated extraction kicker impedance of 25 kΩ/m. Therefore we conclude that this instability is driven by the extraction kicker impedance and expect to be well below threshold in nominal conditions.

A fast instability with growth time of ~100 μs and central frequency in the 60-80 MHz range was observed. This instability is consistent with an electron-proton instability driven by buildup of an electron cloud.

In addition, the resistive wall instability was observed by operating with transverse tunes below the integer (5.81, 5.80) rather than at the nominal tunes of 6.23, 6.20. The observed growth rate is consistent with the estimated resistive-wall impedance.

When these results are scaled to nominal operating conditions (bunched beam, non-zero chromaticity, 1 msec accumulation) we expect to be below threshold for all three of these instability mechanisms.

Target Commissioning

The first beam on target, the first observation of neutrons at SNS, and demonstration of the SNS project completion goals were achieved on April 28, 2006. Figure 11 shows a compilation of beam and neutronics data captured on one of the first beam pulses to the target. The upper left plot shows data from a beam current monitor in the RTBT, the upper right shows the beam image on a temporary view screen mounted to the target, and the lower left shows a neutron time of flight spectrum. Beam pulses as high as 1.6×10^{13} protons/pulse were delivered to the target to satisfy the DOE CD-4 project completion requirement of at least 1×10^{13} protons/pulse accumulated and delivered to the target.

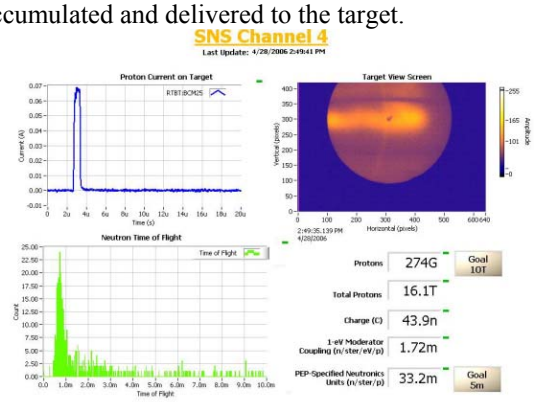

Figure 11: Beam and neutronics data obtained during first beam on target. Shown are a beam current monitor trace (upper left), beam image on the target view screen (upper right) and neutron time-of-flight spectrum (lower left).

REFERENCES

[1] C. Prior et. al., Proc. PAC 2003, p. 1527
[2] N. Holtkamp, Proc. PAC 2003, p. 11
[3] A. Aleksandrov, Proc. PAC 2003, p. 65
[4] D. Jeon, Proc. PAC 2003, p. 107
[5] J. Wei, Proc. PAC 2003, p.571
[6] R.F. Welton et. al., Proc. PAC 2005, p. 472
[7] I.E. Campisi, Proc. PAC 2005, p. 34
[8] S. Assadi, Proc. PAC 2003, p. 498.
[9] A. Feschenko et. al., Proc. LINAC 2004, p. 408.
[10] S. Assadi et. al., Proc. PAC 2003, p. 2706.
[11] J. Galambos et. al., Proc. PAC 2005 p. 79.
[12] J. Galambos, these proceedings
[13] B. Schnizer, Part. Acc. 2 (1971) 141.
[14] C.K. Allen et. al., Proc. PAC 2003, p. 3527.
[15] A. Aleksandrov, Proc. PAC 2005, p. 97
[16] J. Galambos et. al., Proc. PAC 2005, p. 1491.
[17] A. Feschenko et. al., Proc. PAC 2005, p. 3064.
[18] S. Henderson et. al., PAC 2005, p. 3423.
[19] V. Danilov et. al., these proceedings
[20] H. Hahn, Phys. Rev. ST Accel. Beams **7**, 103501 (2004)